

An Information-Theoretic Perspective on Successive Cancellation List Decoding and Polar Code Design

Mustafa Cemil Coşkun, *Student Member, IEEE*, Henry D. Pfister, *Senior Member, IEEE*

Abstract—This work identifies information-theoretic quantities that are closely related to the required list size on average for successive cancellation list (SCL) decoding to implement maximum-likelihood decoding over general binary memoryless symmetric (BMS) channels. It also provides upper and lower bounds for these quantities that can be computed efficiently for very long codes. For the binary erasure channel (BEC), we provide a simple method to estimate the mean accurately via density evolution. The analysis shows how to modify, e.g., Reed-Muller codes, to improve the performance when practical list sizes, e.g., $L \in [8, 1024]$, are adopted. Exemplary constructions with block lengths $N \in \{128, 512\}$ outperform polar codes of 5G over the binary-input additive white Gaussian noise channel.

It is further shown that there is a concentration around the mean of the logarithm of the required list size for sufficiently large block lengths, over discrete-output BMS channels. We provide the probability mass functions (p.m.f.s) of this logarithm, over the BEC, for a sequence of the modified RM codes with an increasing block length via simulations, which illustrate that the p.m.f.s concentrate around the estimated mean.

Index terms— Successive cancellation list decoding, Reed-Muller codes, polar codes, dynamic frozen bits, code design.

I. INTRODUCTION

Polar codes constitute the first deterministic construction of capacity-achieving codes for binary memoryless symmetric (BMS) channels with an efficient decoder [2]. While they achieve capacity under successive cancellation (SC) decoding, their initial performance was not competitive with low-density parity-check (LDPC) and Turbo codes. This changed with the advent of successive cancellation list (SCL) decoding and the addition of cyclic redundancy check (CRC) outer codes [3]. Due to their competitive performance for short block lengths [4], they have been adopted by the 5G standard [5].

This paper was presented in part at the IEEE International Conference on Signal Processing and Communications, July 2020, Bangalore, India [1].

Mustafa Cemil Coşkun is with the Institute for Communications Engineering (LNT), Technical University of Munich, Munich, Germany (email: mustafa.coskun@tum.de). Parts of this work were carried out when he was also with the Institute of Communications and Navigation of the German Aerospace Center (DLR), Weßling, Germany, and with the Department of Electrical and Computer Engineering, Duke University, Durham, USA.

Henry D. Pfister is with the Department of Electrical and Computer Engineering, Duke University, Durham, USA (email: henry.pfister@duke.edu).

The work of M. C. Coşkun was supported in part by the Helmholtz Gemeinschaft through the HGF-Allianz DLR@Uni project Munich Aerospace via the research grant “Efficient Coding and Modulation for Satellite Links with Severe Delay Constraints” and in part by the German Research Foundation (DFG) under Grant KR 3517/9-1. The work of H. D. Pfister was supported in part by the National Science Foundation under Grant No. 1718494. Any opinions, findings, conclusions, and recommendations expressed in this material are those of the authors and do not necessarily reflect the views of these sponsors.

Many authors have optimized polar codes and their variants to improve their performance for SCL decoding [6]–[14].

An important property of SCL decoding is that its performance matches the maximum-likelihood (ML) decoder if the list size is sufficiently large. This work is motivated by the theoretical question: “What list size suffices to approach ML decoding performance for a given channel quality?”. Simulating SCL decoding with a large list size is infeasible for long codes and doesn’t provide much insight into designing codes for SCL decoding. Current works rely mostly on heuristics, e.g., see [7]–[9], [11], [13].

By noting that SCL decoding operates sequentially in N stages, where N is the block length, we identify information-theoretic quantities associated with the required list size on average. For general BMS channels, we provide upper and lower bounds that can be computed efficiently even for very long codes. Our analysis suggests new code design criterion for SCL decoding with practical list sizes, e.g., $L \in [8, 1024]$ by modifying, e.g., Reed-Muller (RM) codes [15], [16]. This is illustrated via exemplary constructions for short- to moderate-length regime, e.g., $N \in \{128, 512\}$, which outperform polar codes of the 5G standard. For the binary erasure channel (BEC), we provide a simple Markov chain approximation to compute the mean using only density evolution and simulations show that it is quite accurate.

Motivated by the numerical results of [1], we show that, for discrete-output BMS channels, the logarithm of required list size at each decoding stage concentrates around the mean for large block lengths using techniques similar to those for analyzing LDPC codes [17], [18]. Over the BEC, we provide its probability mass function (p.m.f.) for modified RM codes with several block lengths. Simulations illustrate the fact that, with increasing block lengths, the p.m.f.s concentrate around the estimated mean.

The paper is organized as follows. In Section II, we provide the preliminaries needed for the rest of the work. In Section III, we introduce the key quantities and use them to analyze the considered list decoders. The convergence properties are studied for general BMS channels as well as for the BEC in Section IV. Numerical results are presented in Section V for the binary-input additive white Gaussian noise (BIAGWN) channel and the BEC. Conclusions follow in Section VI.

II. BACKGROUND

Random variables (r.v.s) are denoted by upper case letters, e.g., X , and their realizations by the lower case counterparts, e.g., x . Random vectors are denoted by $X_i^j =$

$(X_i, X_{i+1}, \dots, X_j)$ and their realizations by x_i^j . If $j < i$, then X_i^j is void. We use $[N]$ for the set $\{1, 2, \dots, N\}$. Subvectors with indices in $\mathcal{S} \subseteq [N]$ are denoted by $x_{\mathcal{S}} = (x_{i_1}, \dots, x_{i_{|\mathcal{S}|}})$ where $i_1 < \dots < i_{|\mathcal{S}|}$ enumerates the elements in \mathcal{S} with $|\mathcal{S}|$ being the cardinality of the set \mathcal{S} . We use $x_{\sim i}$ for the vector $x_{[N] \setminus \{i\}}$. Bold capital letters are used for matrices, e.g., \mathbf{X} .

Consider a BMS channel with binary input $X \in \{0, 1\}$ and general output $Y \in \mathcal{Y}$, i.e., $W : X \rightarrow Y$. The transition probabilities are given by $W(y|x) \triangleq \Pr(Y = y|X = x)$.

A. Polar and Reed-Muller Codes

The polar transform of length $N = 2^n$ is denoted by $\mathbf{G}_N \triangleq \mathbf{B}_N \mathbf{G}_2^{\otimes n}$, where \mathbf{B}_N is the $N \times N$ bit-reversal matrix [2, Sec. VII.B] and $\mathbf{G}_2^{\otimes n}$ is the n -fold Kronecker product of the 2×2 binary Hadamard matrix

$$\mathbf{G}_2 \triangleq \begin{bmatrix} 1 & 0 \\ 1 & 1 \end{bmatrix}.$$

This is the key building block in Arikan's polar codes [2] and RM codes [15], [16].

To define an (N, K) polar or RM code, one partitions the input vector into sub-vectors that carry information and frozen bits whose values are known by the receiver. The set of information and frozen indices are denoted, respectively, by $\mathcal{A} \subseteq [N]$ with $|\mathcal{A}| = K$, and $\mathcal{F} \triangleq [N] \setminus \mathcal{A}$. Thus, the input vector u_1^N can be split into information bits $u_{\mathcal{A}}$ and frozen bits $u_{\mathcal{F}}$. Then, the codeword $x = u\mathbf{G}_N$ is transmitted over the channel. This construction enables efficient SC decoding [2], [19]. For polar codes, the set \mathcal{A} is chosen to minimize a tight upper bound on the error probability under SC decoding; however, the set \mathcal{A} for an r -th order RM code of length N , denoted by $\text{RM}(r, n)$, consists of the indices of rows in \mathbf{G}_N with the Hamming weight at least equal to 2^{n-r} .

B. Successive Cancellation Decoding

Let y_1^N be observations of the bits x_1^N through N copies of the BMS channel W . SC decoding takes the following steps sequentially from $i = 1$ to $i = N$. If $i \in \mathcal{F}$, it sets \hat{u}_i to its frozen value. If $i \in \mathcal{A}$, it computes the soft estimate $p_i(\hat{u}_1^{i-1}) \triangleq \Pr(U_i = 1|Y_1^N = y_1^N, U_1^{i-1} = \hat{u}_1^{i-1})$, and makes a hard decision accordingly as

$$\hat{u}_i = \begin{cases} 0 & \text{if } p_i(\hat{u}_1^{i-1}) < \frac{1}{2} \\ 1 & \text{otherwise.} \end{cases}$$

To understand SC decoding, we focus on the effective channels seen by each of the input bits in u_1^N [2]. SC decoding uses the entire y_1^N vector and all past decisions \hat{u}_1^{i-1} to generate the soft estimate $p_i(\hat{u}_1^{i-1})$ and the hard decision \hat{u}_i for u_i . Let $W_N^{(i)}$ denote the effective (virtual) channel seen by u_i during SC decoding [2]. If all past bits u_1^{i-1} are provided by a genie, then this channel is easier to analyze. The effective channel $W_N^{(i)} : U_i \rightarrow (Y_1^N, U_1^{i-1})$ is then defined by its transition probabilities

$$W_N^{(i)}(y_1^N, u_1^{i-1} | u_i) \triangleq \sum_{u_{i+1}^N \in \{0, 1\}^{N-i}} \frac{1}{2^{N-1}} W_N(y_1^N | u_1^N \mathbf{G}_N)$$

where $W_N(y_1^N | x_1^N) \triangleq \prod_{i=1}^N W(y_i | x_i)$.

C. Successive Cancellation List Decoding

SCL decoding of RM codes (and related subcodes) was introduced in [20]. It was then extended to optimized constructions of generalized concatenated codes in [19]. These approaches became popular after [3] applied them to polar codes that were combined with an outer CRC code to improve their finite-length performance.

SCL decoding recursively computes $Q_i(\tilde{u}_1^i, y_1^N)$, which is proportional to $\Pr(U_1^i = \tilde{u}_1^i, Y_1^N = y_1^N)$ for $i = 1, \dots, N$ via the SC message passing rules for partial input sequences $\tilde{u}_1^i \in \mathcal{U}_i \subseteq \{0, 1\}^i$, which are also called decoding paths. Discarding y_1^N for the ease of notation, we refer to $Q_i(\tilde{u}_1^i)$ as the *myopic likelihood* of the sequence \tilde{u}_1^i as it does not use the receiver's knowledge of frozen bits after u_i .

Let $\mathcal{U}_{i-1} \subseteq \{0, 1\}^{i-1}$ be a subset satisfying $|\mathcal{U}_{i-1}| = L$ and assume that $Q_{i-1}(\tilde{u}_1^{i-1})$ is known for some $\tilde{u}_1^{i-1} \in \mathcal{U}_{i-1}$. Then, for $\tilde{u}_i \in \{0, 1\}$, one can write

$$Q_i(\tilde{u}_1^i) \propto \Pr(U_1^i = \tilde{u}_1^i, Y_1^N = y_1^N) \\ \propto Q_{i-1}(\tilde{u}_1^{i-1}) \Pr(U_i = \tilde{u}_i | Y_1^N = y_1^N, U_1^{i-1} = \tilde{u}_1^{i-1}) \quad (1)$$

where the right-most term can be computed efficiently by the SC decoder starting from $Q_0(\tilde{u}_1^0) \triangleq 1$. This results in $Q_i(\tilde{u}_1^i)$ values for $2L$ partial sequences produced from \mathcal{U}_{i-1} . One then prunes the list down to L sequences by keeping only most likely paths according to (1) for SCL decoding with list size L . Note that if u_i is frozen, then the decoder simply extends all paths with correct frozen bit. After the N -th decoding stage, the estimate \hat{u}_1^N is chosen as the candidate maximizing the function $Q_N(\tilde{u}_1^N)$.

For the BEC, all partial input sequences $u_1^i \in \{0, 1\}^i$ with $Q_i(u_1^i) > 0$ are equiprobable. Hence, for a given u_1^{i-1} , we have $p_i(u_1^{i-1}) \in \{0, 1/2, 1\}$. If $p_i(u_1^{i-1}) \in \{0, 1\}$, then u_i is known perfectly at the receiver. However, if $p_i(u_1^{i-1}) = 1/2$ and u_i is not frozen, then \hat{u}_i can be seen as an erasure. When an information bit is decoded to an erasure, it is replaced by both possible values (assuming the list size is large enough) and decoding proceeds separately under these two hypotheses. The number of hypotheses (i.e., partial input sequences) is halved if the decoded value for a frozen bit contradicts with its actual value for different partial input sequences [21, Appendix A]. An error is declared if, at any decoding stage, the number of hypotheses exceeds L or if there are more than one hypothesis at the end of the process, i.e., if $\exists \tilde{u}_1^N \in \{0, 1\}^N$, $\tilde{u}_1^N \neq u_1^N$ with $Q_N(\tilde{u}_1^N) > 0$.

D. Successive Cancellation Inactivation Decoding

Successive cancellation inactivation (SCI) decoding is a more efficient version of SCL decoding for the BEC proposed in [22]. It follows the same decoding schedule as SCL decoding but instead replaces an erased information bit by a variable, i.e., the bit is *inactivated* [23]–[25]. Later, the decoding function for any frozen bit provides a linear equation if its output is not an erasure [22, Eq. (3)]. Thanks to this equation, the inactivated bit may be resolved. This can be done at any stage of the decoding process when the obtained equation is not a trivial one or delayed until the end. When a dummy variable is eliminated without delaying to the end

of decoding, we refer to this as a *consolidation* event. In this work, our focus is on SCI decoding with consolidations.

SCI decoding can inactivate multiple bits if required. If the maximum number of inactivations is not bounded, then it implements ML decoding. For further details, see [22].

E. Dynamic Frozen Bits

An important observation in [6] is that decoders having the successive nature (e.g., SCL decoding) still work (with slight modifications) even if, for some $i \in \mathcal{F}$, the bit u_i is a function of a set of preceding information bits. A frozen bit whose value depends on past inputs is called dynamic.

A polar code with dynamic frozen bits is defined by its information indices \mathcal{A} and a matrix that defines each frozen bit as a linear combination of preceding information bits. There are now a number of approaches for choosing \mathcal{A} and dynamic frozen bit constraints, e.g., [6]–[8], [13], [14], which aim at having a resulting code with large minimum distance and/or small multiplicity of minimum weight codewords as well as low to moderate decoding complexity for target block error rates (BLERs). In this work, after specifying \mathcal{A} , we define each frozen bit to be a uniform random linear combination of information bits preceding it.

III. ANALYSIS OF THE LIST DECODERS

An important property of list decoding is that, if the correct codeword is on the list at the end of decoding, then the error probability is upper bounded by that of ML decoding. We study how large the list should be at each stage so that the correct codeword is likely to be on the list.

A. An Information-Theoretic Perspective

Consider a length- N polar code with SCL decoding after the m -th decoding stage. Since SCL decoding does not use future frozen bits, we focus on the subset of length- m input sequences that have significant conditional entropy given the channel observation. An important insight is that, after observing Y_1^N , the uncertainty in U_1^m is quantified by the entropy

$$H(U_1^m | Y_1^N) = \sum_{i=1}^m H(U_i | U_1^{i-1}, Y_1^N) \quad (2)$$

where U_1^N is assumed to be uniform over $\{0, 1\}^N$. This is exactly true if the first m bits are all information bits, i.e., if $[m] \subseteq \mathcal{A}$. If $[m]$ contains also frozen indices, however, then the situation is more complicated.¹

Let $\mathcal{A}^{(m)} \triangleq \mathcal{A} \cap [m]$ and $\mathcal{F}^{(m)} \triangleq \mathcal{F} \cap [m]$ be the sets containing information and frozen indices within the first m input bits, respectively. Now consider an experiment where the frozen bits U_i with $i \in \mathcal{F}^{(m)}$ are uniform and independent of U_1^{i-1} . Using (2) naively with the assumption that $U_{\mathcal{F}^{(m)}}$ is not known to the receiver would cause an overestimate of $H(U_1^m | Y_1^N)$ by an amount of at least $\sum_{i \in \mathcal{F}^{(m)}} H(U_i | U_1^{i-1}, Y_1^N)$. In

¹Here, it is assumed that the frozen bits $U_{\mathcal{F}}$ are also uniformly distributed and SCL decoding learns them causally. In the case of dynamic frozen bits, uniform random constants are added, which are revealed causally as in the case of other frozen bits.

addition to this, the frozen bits $U_{\mathcal{F}^{(m)}}$ may reveal additional information about the previous information bits.

To better understand the uncertainty within the first m input bits during SCL decoding, we define the quantity

$$d_m(y_1^N) \triangleq H(U_{\mathcal{A}^{(m)}} | Y_1^N = y_1^N, U_{\mathcal{F}^{(m)}}) \quad (3)$$

and the corresponding r.v. is denoted as D_m that takes on the value $d_m(y_1^N)$ when $Y_1^N = y_1^N$. Note that the mean of D_m corresponds to the conditional entropy, i.e.,

$$\bar{D}_m \triangleq \mathbb{E}[d_m(Y_1^N)] = H(U_{\mathcal{A}^{(m)}} | Y_1^N, U_{\mathcal{F}^{(m)}})$$

and we define a difference sequence as

$$\Delta_m \triangleq \bar{D}_m - \bar{D}_{m-1}.$$

Observe that, if U_m is an information bit, then we have

$$\begin{aligned} \Delta_m &= H(U_{\mathcal{A}^{(m)}} | Y_1^N, U_{\mathcal{F}^{(m)}}) - H(U_{\mathcal{A}^{(m-1)}} | Y_1^N, U_{\mathcal{F}^{(m-1)}}) \\ &= H(U_{\mathcal{A}^{(m)}} | Y_1^N, U_{\mathcal{F}^{(m-1)}}) - H(U_{\mathcal{A}^{(m-1)}} | Y_1^N, U_{\mathcal{F}^{(m-1)}}) \\ &= H(U_{\mathcal{A}^{(m)}}, U_{\mathcal{F}^{(m-1)}} | Y_1^N) - H(U_{\mathcal{A}^{(m-1)}}, U_{\mathcal{F}^{(m-1)}} | Y_1^N) \\ &= H(U_1^{m-1} | Y_1^N) + H(U_m | Y_1^N, U_1^{m-1}) - H(U_1^{m-1} | Y_1^N) \\ &= H(U_m | Y_1^N, U_1^{m-1}) \end{aligned} \quad (4)$$

which is exactly what one would expect from the naive analysis given by (2).

If U_m is a frozen bit, then consider a model where it is not known to the receiver at the time of transmission.² The act of revealing U_m to the receiver changes the conditional uncertainty about $U_{\mathcal{A}^{(m-1)}}$ by

$$\begin{aligned} \Delta_m &= H(U_{\mathcal{A}^{(m)}} | Y_1^N, U_{\mathcal{F}^{(m)}}) - H(U_{\mathcal{A}^{(m-1)}} | Y_1^N, U_{\mathcal{F}^{(m-1)}}) \\ &= H(U_{\mathcal{A}^{(m-1)}} | Y_1^N, U_{\mathcal{F}^{(m-1)}}, U_m) - H(U_{\mathcal{A}^{(m-1)}} | Y_1^N, U_{\mathcal{F}^{(m-1)}}) \\ &= -I(U_m; U_{\mathcal{A}^{(m-1)}} | Y_1^N, U_{\mathcal{F}^{(m-1)}}) \\ &= H(U_m | Y_1^N, U_1^{m-1}) - H(U_m | Y_1^N, U_{\mathcal{F}^{(m-1)}}) \\ &\geq H(U_m | Y_1^N, U_1^{m-1}) - 1. \end{aligned} \quad (5)$$

This expression quantifies the effect of revealing the new frozen bit as a reduction in the conditional entropy of the information bits preceding it. A large reduction may occur when the channel $W_N^{(m)}$ has low entropy (i.e., a low-entropy effective channel is essentially frozen) and the reduction will be small if the channel entropy is high (i.e., the input is unpredictable from Y_1^N and U_1^{m-1}).

For BMS channels, we can combine (4) and (5) to understand the dynamics of \bar{D}_m . This gives a proxy for the uncertainty in SCL decoding after m steps. We have

$$\sum_{i \in \mathcal{A}^{(m)}} H(W_N^{(i)}) - \sum_{i \in \mathcal{F}^{(m)}} (1 - H(W_N^{(i)})) \leq \bar{D}_m \quad (6a)$$

$$\leq \sum_{i \in \mathcal{A}^{(m)}} H(W_N^{(i)}) \quad (6b)$$

The lower bound assumes that frozen bits (when perfectly observed) always reduce the entropy.

²This reflects how SCL decoding operates, i.e., it does not use the knowledge of any frozen bit U_m until reaching the end of its decoding stage m . The soft estimate $p_m(u_1^{m-1})$ provides an additional information to separate the hypotheses (i.e., paths) although the hard estimate is chosen as $\hat{u}_m = u_m$ independent of $p_m(u_1^{m-1})$.

Theorem 1. Upon observing y_1^N when u_1^N is transmitted, the set of partial sequences \tilde{u}_1^m with a larger likelihood than some fraction of that for true sequence u_1^m after m stages of SCL decoding is given by

$$\mathcal{S}_\alpha^{(m)}(u_1^m, y_1^N) \triangleq \{\tilde{u}_1^m : Q_m(\tilde{u}_1^m) \geq \alpha Q_m(u_1^m)\}$$

where the fraction is given by a positive number $\alpha \leq 1$. On average, the logarithm of its cardinality is upper bounded by

$$\begin{aligned} \mathbb{E} \left[\log_2 |\mathcal{S}_\alpha^{(m)}| \right] &\leq \bar{D}_m + \log_2 \alpha^{-1} \\ &= H(U_{\mathcal{A}^{(m)}} | Y_1^N, U_{\mathcal{F}^{(m)}}) + \log_2 \alpha^{-1}. \end{aligned} \quad (7)$$

Proof. Assume, w.l.o.g., that u_1^N and y_1^N are transmitted and observed, respectively. Then, we have

$$\begin{aligned} \log_2 |\mathcal{S}_\alpha^{(m)}| &\stackrel{(a)}{=} \log_2 \sum_{\tilde{u}_1^m} \mathbb{1}_{(p(\tilde{u}_{\mathcal{A}^{(m)}} | y_1^N, u_{\mathcal{F}^{(m)}}) \geq \alpha \cdot p(u_{\mathcal{A}^{(m)}} | y_1^N, u_{\mathcal{F}^{(m)}}))} \\ &\stackrel{(b)}{\leq} -\log_2 \alpha \cdot p(u_{\mathcal{A}^{(m)}} | y_1^N, u_{\mathcal{F}^{(m)}}) \end{aligned}$$

where (a) follows from $Q_m(u_1^m) \propto \Pr(U_1^m = \tilde{u}_1^m, Y_1^N = y_1^N)$ and Bayes' rule and (b) from the fact that if there are more than $(\alpha \cdot p(u_{\mathcal{A}^{(m)}} | y_1^N, u_{\mathcal{F}^{(m)}}))^{-1}$ sequences $\tilde{u}_{\mathcal{A}}$ with probability $\alpha \cdot p(u_{\mathcal{A}^{(m)}} | y_1^N, u_{\mathcal{F}^{(m)}})$, then the total probability exceeds 1. As the inequality is valid for any pair u_1^N and y_1^N , taking the expectation over all u_1^m and y_1^N yields the stated result. \square

Note that α is used as a tuning parameter to catch near misses. Making it too small will keep many partial sequences with low probabilities in the set while choosing it as $\alpha = 1$ will exclude the decoding paths with probabilities close to the correct one. For Monte-Carlo simulations validating (7), α is chosen close to 1, but still keeping $\mathbb{E} \left[\log_2 |\mathcal{S}_\alpha^{(m)}| \right]$ close to \bar{D}_m especially for small values of m .

Now, consider SCL decoding whose list size is L_m during the m -th decoding step. Then, the decoder should satisfy $L_m \geq |\mathcal{S}_1^{(m)}|$ for the true u_1^m to be in the set $\mathcal{S}_1^{(m)}$. Using (7) and (6b) yields the simple upper bound

$$\mathbb{E} \left[\log_2 |\mathcal{S}_\alpha^{(m)}| \right] \leq \sum_{i \in \mathcal{A}^{(m)}} H(W_N^{(i)}) + \log_2 \alpha^{-1}. \quad (8)$$

Remark 1. The analysis in terms of $\log_2 L_m$ has two weaknesses. First, the entropy \bar{D}_m only characterizes typical events, e.g., ensuring that the correct codeword stays on the list at least half of the time, whereas coding typically focuses on rarer events, e.g., BLERs less than 10^{-2} . Second, the sequence \bar{D}_m is averaged over Y_1^N but the actual decoder sees a random realization $d_m(y_1^N) = H(U_{\mathcal{A}^{(m)}} | Y_1^N = y_1^N, U_{\mathcal{F}^{(m)}})$. Nevertheless, we believe the results provide a useful step towards a theoretical analysis of SCL decoding. The numerical results in Section V illustrate the accuracy of the analysis. To motivate the analysis further, we study the convergence properties of the r.v. D_m in Section IV.

Remark 2. The results have significance for code design. To achieve good performance under SCL decoding whose list size is L_m during the m -th decoding step, a reasonable first-order design criterion is that $\log_2 L_m \geq \bar{D}_m$. This observation implies, in principle, that frozen bits should be allocated to prevent \bar{D}_m from exceeding $\log_2 L_m$. Since computing \bar{D}_m

requires simulations with huge list sizes (if not unbounded) and the upper bound (6b) ignores the affect of frozen bits, we use the lower bound (6a) as the proxy for designs. Motivated by the observations of Remark 1, we believe that a relatively low signal-to-noise ratio (SNR) values should be chosen for the analysis in order to capture rare events. Using these guidelines, exemplary designs are provided in Section V-A.

B. The Binary Erasure Channel

Proposition 1. On the BEC, the list of all valid partial input sequences u_1^m generated by SCL decoding with unbounded list size upon observing y_1^N form an affine subspace, denoted as $\mathcal{S}^{(m)}(y_1^N)$.

Proof. Let \mathcal{E} denote the set of erased positions in the realization y_1^N . Then, we can write

$$(u_{\mathcal{A}^{(m)}}, u_{m+1}^N) \mathbf{G}'_{[N] \setminus \mathcal{F}^{(m)}} = y_{[N] \setminus \mathcal{E}} \oplus u_{\mathcal{F}^{(m)}} \mathbf{G}'_{\mathcal{F}^{(m)}} \quad (9)$$

where $\mathbf{G}'_{\mathcal{S}}$ is the matrix formed by the rows of \mathbf{G}_N indexed in \mathcal{S} and then removing its columns indexed in \mathcal{E} and \oplus is the bit-wise XOR of two vectors. This equation enables to use the frozen bits $u_{\mathcal{F}^{(m)}}$ as side information. Let \mathcal{C} denote the set of all possible solutions for $(u_{\mathcal{A}^{(m)}}, u_{m+1}^N)$, which is an affine subspace. We are interested in all compatible partial information sequences $u_{\mathcal{A}^{(m)}}$ with (9) (hence, u_1^m as $u_{\mathcal{F}^{(m)}}$ is a linear transform of $u_{\mathcal{A}^{(m)}}$). To this end, we define the mapping $\Pi_{\mathcal{A}^{(m)}} : \mathbb{F}_2^{N-|\mathcal{F}^{(m)}|} \rightarrow \mathbb{F}_2^{|\mathcal{A}^{(m)}|}$ as

$$\Pi_{\mathcal{A}^{(m)}}(\mathcal{C}) \triangleq \left\{ v_1^{|\mathcal{A}^{(m)}|} : v_1^{N-|\mathcal{F}^{(m)}|} \in \mathcal{C} \right\}$$

which is a linear mapping since it can be represented as a multiplication of the input by a matrix formed by stacking an $|\mathcal{A}^{(m)}| \times |\mathcal{A}^{(m)}|$ identity matrix and an $(N-m) \times |\mathcal{A}^{(m)}|$ all-zero matrix. Then, the result follows by noting that a linear transform of an affine subspace is affine. \square

Let $L_m(y_1^N)$ denote the list length after m -th decoding stage of SCL decoding with unbounded list size, i.e., $L_m(y_1^N) = |\mathcal{S}^{(m)}(y_1^N)|$. Since each member of the list is equally likely, the proposition provides an immediate corollary, which follows from the definition (3) and observing that a subspace dimension is always a non-negative integer. The corollary bridges between the introduced quantity $d_m(y_1^N)$ and the list length $L_m(y_1^N)$ SCL decoding with unbounded list size explicitly.

Corollary 1. At any decoding stage m , the list length $L_m(y_1^N)$, $y_1^N \in \{0, ?, 1\}^N$, of SCL decoding satisfies

$$\log_2 L_m(y_1^N) = d_m(y_1^N).$$

Hence, $L_m(y_1^N)$ is a non-negative integer power of 2.

Next, another corollary is provided, which follows from the fact that $L_m(y_1^N)$ is a non-negative integer power of 2 in combination with the error events of SCL decoding with a fixed list size L defined in Section II-C, i.e., either $|\mathcal{S}^{(m)}(y_1^N)| > L$ for any $m \in [N]$ or $|\mathcal{S}^{(N)}(y_1^N)| \neq 1$.

Corollary 2. SCL decoding with the list size L performs the same as SCL decoding with $L' = 2^{\lceil \log_2 L \rceil}$.

The question of “how large should the list size be for ML decoding?” was partially addressed by [26, Thm. 1] for the case of the BEC by providing an upper bound. We improve this bound with the following lemma.

Lemma 1. *Let $L^*(\mathcal{C})$ be the smallest list size for SCL decoding that implements ML decoding for an (N, K) binary linear code \mathcal{C} . Let ζ and γ denote the index of the last frozen bit before the first information bit, and the last (dynamic) frozen bit when \mathcal{C} is represented as a polar code (with dynamic frozen bits), i.e.,*

$$\zeta \triangleq \min \mathcal{A} \quad \text{and} \quad \gamma \triangleq \max \mathcal{F}.$$

Then $L^*(\mathcal{C})$ is upper bounded as

$$L^*(\mathcal{C}) \leq \min \left\{ 2^{N(1-R) - (\zeta - 1)}, 2^{\gamma - N(1-R)} \right\} \quad (10)$$

where R is the code rate.

Proof. Observe that the first $\zeta - 1$ frozen bits are of no use for pruning paths. Hence, there are $N(1 - R) - (\zeta - 1)$ frozen bits, which have the potential to prune half of the existing paths. If there are more than $2^{N(1-R) - (\zeta - 1)}$ paths at any decoding stage during SCL decoding, then there will be at least 2 solutions at the end.

We refer the reader to [26, Thm. 1], which states that $L^*(\mathcal{C}) \leq 2^{\gamma - N(1-R)}$, concluding the proof. \square

Note that [26, Thm. 1] states that $L^*(\mathcal{C}) \leq 2^{\gamma - N(1-R)}$, which is usually relevant for low rate codes as $N(1 - R)$ is large. Depending on the allocation of the frozen bit indices, (10) can improve the previous result significantly. Consider, for instance, RM(5, 7) with parameters $N = 128$ and $K = 120$ where $\zeta = 4$ and $\gamma = 65$. The previous result states that $L^* \leq 2^{57}$ while (10) gives $L^* \leq 2^5$. Hence, Lemma 1 usually tightens the bound for high-rate codes. However, even this bound is far from being practical, especially for codes with rates $R \approx 0.5$. Consider, for instance, RM(3, 7), where (10) gives $L^* \leq 2^{49}$. In addition, the bounds are obviously independent of the channel quality since they are interested in exact ML decoding. If ϵ is very low then one requires much shorter lists on average to decode successfully.

Recall that SCL decoding branches out the paths not for each information bit but whenever necessary. Instead, information bits are inactivated whenever necessary in the case of SCI decoding. Therefore, we study the dynamics of SCI decoding with consolidations without any constraints on the subspace dimension, which is equivalent to SCL decoding with unbounded list size. This relaxation gives more understanding on the complexity vs. performance trade-offs on average. Its practical relevance stems from the complexity-adaptive nature of the decoders for the case of the BEC. Recalling Corollary 1, observe that SCI decoding provides a concrete example of the information-theoretic perspective since, for any y_1^N , the subspace dimension is $d_m(y_1^N) = H(U_{\mathcal{A}(m)} | Y_1^N = y_1^N, U_{\mathcal{F}(m)})$ and SCI decoding stores a basis for this subspace instead of listing all possible sequences in it.

Let $\epsilon_N^{(m)} \triangleq \Pr(p_m(u_1^{m-1}) = 1/2)$, where the implied randomness is due to the received vector. Consider the decoding of information and frozen bits given the observed vector and

preceding frozen bits. When an information bit u_m is decoded, one of following events occurs:

- The information bit is decoded as an erasure and the subspace dimension increases by one, i.e., $d_m(y_1^N) = d_{m-1}(y_1^N) + 1$. Averaged over all y_1^N , the probability of this event equals $\epsilon_N^{(m)}$ [22].
- The information bit is decoded as an affine function of the previous information bits and the subspace dimension is unchanged, i.e., $d_m(y_1^N) = d_{m-1}(y_1^N)$. Averaged over all y_1^N , the probability of this event equals $1 - \epsilon_N^{(m)}$ [22].

If a frozen u_m is decoded, one of following events occurs:

- The decoder returns an erasure for the frozen bit. In this case, revealing the true value of the frozen bit allows decoding to continue, but no new information is provided about preceding information bits. Thus, we have $d_m(y_1^N) = d_{m-1}(y_1^N)$. Averaged over all y_1^N , the probability of this event equals $\epsilon_N^{(m)}$ [22].
- The frozen bit is decoded as an affine function of the previous information bits. Averaged over all y_1^N , the probability of this event equals $1 - \epsilon_N^{(m)}$ [22]. In this case, revealing the true value of the frozen bit gives a linear equation for a subset of the preceding information bits. If the linear equation is informative, then the subspace dimension decreases by one via a consolidation event, i.e., we have $d_m(y_1^N) = d_{m-1}(y_1^N) - 1$. Otherwise, the dimension is unchanged, i.e., $d_m(y_1^N) = d_{m-1}(y_1^N)$.

At first glance, these rules might appear to tell the whole story. But the erasure rate $\epsilon_N^{(m)}$ is averaged over all y_1^N whereas predicting the value of D_m requires the conditional probability of erasure events given all past observations. More importantly, to understand consolidation events, one needs to compute the probability that the obtained equation is informative.

Since we do not have expressions for these quantities,³ we use two simplifying approximations for a given random sequence D_1, \dots, D_{m-1} . First, we approximate the probability of decoding an erasure for a frozen bit as independent of all past events, i.e., for any $d_1^{m-1} \triangleq (d_1(y_1^N), \dots, d_{m-1}(y_1^N))$, we write

$$\Pr(p_m(u_1^{m-1}) = 1/2 | D_1^{m-1} = d_1^{m-1}) \approx \epsilon_N^{(m)}.$$

Second, we approximate the probability that an informative equation obtained from consolidation at decoding stage m by $1 - 2^{-D_{m-1}}$, independent of sequence D_1, \dots, D_{m-2} . This means, for $m \in \mathcal{F}$, we write

$$\begin{aligned} \Pr(D_m = d_{m-1} | D_1^{m-1} = d_1^{m-1}, p_m(u_1^{m-1}) \neq 1/2) &\approx 2^{-d_{m-1}} \\ &\approx 1 - \Pr(D_m = d_{m-1} - 1 | D_1^{m-1} = d_1^{m-1}, p_m(u_1^{m-1}) \neq 1/2) \end{aligned}$$

which comes from modeling the obtained equation and the subset using a uniform random model. Under these assumptions, the random sequence D_1, \dots, D_N can be modelled by

³Even if we had them exactly, they may be too complicated to be useful.

an inhomogeneous Markov chain with transition probabilities $P_{i,j}^{(m)} \triangleq \Pr(D_m = j \mid D_{m-1} = i)$ where

$$P_{i,j}^{(m)} \approx \begin{cases} \epsilon_N^{(m)} & \text{if } m \in \mathcal{A}, j = i + 1 \\ 1 - \epsilon_N^{(m)} & \text{if } m \in \mathcal{A}, j = i \\ \epsilon_N^{(m)} + (1 - \epsilon_N^{(m)}) 2^{-D_{m-1}} & \text{if } m \in \mathcal{F}, j = i \\ (1 - \epsilon_N^{(m)}) (1 - 2^{-D_{m-1}}) & \text{if } m \in \mathcal{F}, j = i - 1. \end{cases} \quad (11)$$

Consider now decoding of frozen bit u_m based on this Markov chain approximation. We write

$$\begin{aligned} \bar{D}_m &\approx \mathbb{E} \left[D_{m-1} - (1 - \epsilon_N^{(m)}) (1 - 2^{-D_{m-1}}) \right] \\ &\approx \bar{D}_{m-1} - (1 - \epsilon_N^{(m)}) (1 - 2^{-\bar{D}_{m-1}}) \end{aligned} \quad (12)$$

where the last line follows from approximating $\mathbb{E} [2^{-D_m}]$ as $2^{-\bar{D}_m}$. In the case of information bit u_m , we have

$$\begin{aligned} \bar{D}_m &\approx \mathbb{E} \left[\epsilon_N^{(m)} (D_{m-1} + 1) + (1 - \epsilon_N^{(m)}) D_{m-1} \right] \\ &= \bar{D}_{m-1} + \epsilon_N^{(m)}. \end{aligned} \quad (13)$$

By setting $\bar{D}_0 \triangleq 0$, (12) and (13) give the simple recursive approximation

$$\bar{D}_m \approx \begin{cases} \bar{D}_{m-1} + \epsilon_N^{(m)} & \text{if } m \in \mathcal{A} \\ \bar{D}_{m-1} - (1 - \epsilon_N^{(m)}) (1 - 2^{-\bar{D}_{m-1}}) & \text{if } m \in \mathcal{F}. \end{cases} \quad (14)$$

IV. CONCENTRATION FOR LIST DECODERS

This section studies the stochastic convergence properties of the r.v. D_m . In particular, we show that the required uncertainty, quantified by D_m , accumulated by SCL decoding to keep the correct path on the list concentrates around its mean \bar{D}_m for sufficiently large block lengths.

A. General Approach

We form a Doob's Martingale by sequentially revealing information about the object of interest (e.g., see [17], [18]), which is the conditional entropy in our case. In N consecutive steps, we reveal the random channel realizations. Irrespective of the revealed realization, the change in the conditional entropy is bounded by some constant. This lets us use the Azuma-Hoeffding inequality [27, Thm. 12.6] since the channels under consideration are memoryless.

Proposition 2. *The sequence of r.v.s $H_0^{(m)}, H_1^{(m)}, \dots, H_N^{(m)}$ where $H_i^{(m)} \triangleq \mathbb{E} [D_m | Y_1^i]$ is a Doob's Martingale, i.e.,*

$$H_i^{(m)} \text{ is a function of } Y_1^i \quad (15)$$

$$\mathbb{E} [|D_m|] < \infty \quad (16)$$

$$H_{i-1}^{(m)} = \mathbb{E} [H_i^{(m)} | Y_1^{i-1}]. \quad (17)$$

Proof. The statement (15) follows from the construction of r.v.s $H_i^{(m)}$ and the definition of conditional expectation. The inequality (16) follows from the non-negativity of D_m and $\mathbb{E} [D_m] = H(U_{\mathcal{A}^{(m)}} | Y_1^N, U_{\mathcal{F}^{(m)}})$. Finally, (17) follows by

$$\mathbb{E} [H_i^{(m)} | Y_1^{i-1}] = \mathbb{E} [\mathbb{E} [D_m | Y_1^i] | Y_1^{i-1}] \quad (18)$$

$$= \mathbb{E} [D_m | Y_1^{i-1}] \quad (19)$$

$$= H_{i-1}^{(m)} \quad (20)$$

where (18) and (20) follow from the definition of $H_i^{(m)}$, and (19) from the tower property [28, Eq. (C.13)]. \square

Proposition 3. *Consider transmission over a discrete output BMS channel satisfying $W(y|x) \geq \delta > 0, \forall y \in \mathcal{Y}, \forall x \in \{0, 1\}$. Then, for all $i \in [N]$ and all values y_1^N and \tilde{y}_1^N such that $y_{\sim i} = \tilde{y}_{\sim i}$ and $y_i \neq \tilde{y}_i$, the conditional entropy $d_m(y_1^N) = H(U_{\mathcal{A}^{(m)}} | Y_1^N = y_1^N, U_{\mathcal{F}^{(m)}})$ satisfies*

$$|d_m(y_1^N) - d_m(\tilde{y}_1^N)| \leq 4 |\log_2 \delta|. \quad (21)$$

Proof. In the following, the r.v.s are not explicitly written in the probability assignments, e.g., the probabilities are denoted as $p(u_1^m, x_1^N, y_1^N) = \Pr(U_1^m = u_1^m, X_1^N = x_1^N, Y_1^N = y_1^N)$.

The proof starts by writing

$$\begin{aligned} &\frac{p(u_{\mathcal{A}^{(m)}} | y_1^N, u_{\mathcal{F}^{(m)}})}{p(u_{\mathcal{A}^{(m)}} | \tilde{y}_1^N, u_{\mathcal{F}^{(m)}})} \stackrel{(a)}{=} \frac{p(u_1^m, y_1^N)}{p(y_1^N, u_{\mathcal{F}^{(m)}})} \cdot \frac{p(\tilde{y}_1^N, u_{\mathcal{F}^{(m)}})}{p(u_1^m, \tilde{y}_1^N)} \\ &\stackrel{(b)}{=} \frac{\sum_{x_1^N} p(u_1^m, x_1^N, y_1^N)}{\sum_{x_1^N} p(y_1^N, x_1^N, u_{\mathcal{F}^{(m)}})} \cdot \frac{\sum_{x_1^N} p(\tilde{y}_1^N, x_1^N, u_{\mathcal{F}^{(m)}})}{\sum_{x_1^N} p(u_1^m, x_1^N, \tilde{y}_1^N)} \\ &\stackrel{(c)}{=} \frac{\sum_{x_i} W(y_i | x_i) \sum_{x_{\sim i}} p(u_1^m, x_1^N, y_{\sim i})}{\sum_{x_i} W(\tilde{y}_i | x_i) \sum_{x_{\sim i}} p(u_1^m, x_1^N, y_{\sim i})} \\ &\quad \cdot \frac{\sum_{x_i} W(\tilde{y}_i | x_i) \sum_{x_{\sim i}} p(y_{\sim i}, x_1^N, u_{\mathcal{F}^{(m)}})}{\sum_{x_i} W(y_i | x_i) \sum_{x_{\sim i}} p(y_{\sim i}, x_1^N, u_{\mathcal{F}^{(m)}})} \\ &\stackrel{(d)}{=} \frac{\sum_{x_i} W(y_i | x_i) p(u_1^m, x_i, y_{\sim i})}{\sum_{x_i} W(\tilde{y}_i | x_i) p(u_1^m, x_i, y_{\sim i})} \\ &\quad \cdot \frac{\sum_{x_i} W(\tilde{y}_i | x_i) p(y_{\sim i}, x_i, u_{\mathcal{F}^{(m)}})}{\sum_{x_i} W(y_i | x_i) p(y_{\sim i}, x_i, u_{\mathcal{F}^{(m)}})} \end{aligned} \quad (22)$$

where (a) follows from Bayes' rule, (b) and (d) from the law of total probability, and (c) from rearranging the summation, Bayes' rule and noting that Y_i and $(U_1^m, X_{\sim i}, Y_{\sim i})$ are independent given X_i . Then, we take the logarithm and absolute value of both sides in (22). Combining the triangle inequality, i.e., $|a + b| \leq |a| + |b|$, with the fact that each summand is upper bounded by $\max_y |\log_2 W(y|0)|$, e.g.,

$$\left| \log_2 \sum_{x_i} W(y_i | x_i) p(u_1^m, x_i, y_{\sim i}) \right| \leq \max_y |\log_2 W(y|0)|$$

we conclude that

$$\left| \log_2 \frac{p(u_{\mathcal{A}^{(m)}} | y_1^N, u_{\mathcal{F}^{(m)}})}{p(u_{\mathcal{A}^{(m)}} | \tilde{y}_1^N, u_{\mathcal{F}^{(m)}})} \right| \leq 4 \max_y |\log_2 W(y|0)|. \quad (23)$$

Since (23) is valid for any u_1^m , averaging over all u_1^m , combined with the Jensen's inequality, leads to (21) by noting $W(y|0) \geq \delta, \forall y \in \mathcal{Y}$. \square

As a result of Proposition 3, the following corollary provides a concentration for the logarithm of the list size required to approach the performance of a code under ML decoding when the transmission is over discrete output BMS channels. More precisely, the normalized (with respect to the block length) deviation of the logarithm of the random list size, required to

keep the correct codeword in the list, from the average decays exponentially fast.

Corollary 3. *For transmission over a discrete output BMS channel satisfying $W(y|x) \geq \delta > 0, \forall y \in \mathcal{Y}, \forall x \in \{0, 1\}$, the r.v. $D_m, m \in [N]$, concentrates around its mean \bar{D}_m for sufficiently large block lengths, i.e., for any $\beta > 0$, we have*

$$\Pr \left\{ \frac{1}{N} |D_m - \bar{D}_m| > \beta \right\} \leq 2 \exp \left(-\frac{\beta^2}{32 |\log_2 \delta|^2 N} \right). \quad (24)$$

Proof. Since the channel under consideration is memoryless, $Y_i, i \in [N]$, are independent due to the uniform U_1^N . Hence, Proposition 3 implies

$$\left| H_i^{(m)} - H_{i-1}^{(m)} \right| \leq 4 |\log_2 \delta|, \quad i \in [N].$$

The Azuma-Hoeffding inequality [27, Thm. 12.4] is applied then by observing that the first element in the martingale is the expectation of D_m and the last one is the r.v. itself, i.e., $H_0^{(m)} = \bar{D}_m$ and $H_N^{(m)} = D_m$. \square

Since $\delta = 0$ for the BEC, it will be considered separately in the next section. For the case where $W(y|0)$ is a continuous probability density function on a compact set $\mathcal{Y} \subset \mathbb{R}$, the same proof applies with $\delta = \min_{y \in \mathcal{Y}} W(y|0)$. But, the proof does not extend to unbounded output alphabets.

B. The Binary Erasure Channel

SCI decoding over the BEC is equivalent to solving a system of linear equations with side information depending on the decoding stage. In other words, the decoder has the knowledge of the frozen bits $u_{\mathcal{F}^{(m)}}$ after the decoding stage m as side information.

Proposition 4. *For transmission over the BEC, the subspace dimension satisfies the Lipschitz-1 condition: for all $i \in [N]$ and all values y_1^N and \tilde{y}_1^N such that $y_{\sim i} = \tilde{y}_{\sim i}$ and $y_i \neq \tilde{y}_i$, the subspace dimension satisfies*

$$|d_m(y_1^N) - d_m(\tilde{y}_1^N)| \leq 1. \quad (25)$$

Proof. It suffices to consider the case where y_i is not erased, but \tilde{y}_i is an erasure (i.e., $y_i = x_i$ and $\tilde{y}_i = ?$). Recall the linear system given as (9). All compatible vectors $(u_{\mathcal{A}^{(m)}}, u_{m+1}^N)$, $m \in [N]$, with (9) form an affine subspace. The dimension of this subspace is equal to $d'_N(y_1^N) = N - |\mathcal{F}^{(m)}| - \text{rank}(\mathbf{G}'_N)$. Since removing one more column of \mathbf{G}'_N (and also of $\mathbf{G}'_{\mathcal{F}^{(m)}}$) cannot decrease the rank by more than one, we have

$$d'_N(y_1^N) \leq d'_N(\tilde{y}_1^N) \leq d'_N(y_1^N) + 1. \quad (26)$$

Hence, the number of compatible vectors $(u_{\mathcal{A}^{(m)}}, u_{m+1}^N)$ with (9) is (at most) doubled or unchanged.

We are interested in the subspace dimension $d_m(y_1^N)$. This is equal to the number of different subvectors $u_{\mathcal{A}^{(m)}}$ of all compatible $(u_{\mathcal{A}^{(m)}}, u_{m+1}^N)$ with (9). Using (26), one concludes that the number of different vectors $u_{\mathcal{A}^{(m)}}$ either increases by a factor of 2 or does not change, resulting in (25). \square

Corollary 4. *The subspace dimension D_m concentrates around its mean \bar{D}_m for sufficiently large block lengths, i.e., for any $\beta > 0$, we have*

$$\Pr \left\{ \frac{1}{N} |D_m - \bar{D}_m| > \beta \right\} \leq 2 \exp \left(-\frac{\beta^2}{2} N \right). \quad (27)$$

Proof. As for Corollary 3, apply the Azuma-Hoeffding inequality [27, Thm. 12.4] via Proposition 4. \square

Remark 3. *Let $\rho = \lceil \log_2 m \rceil$ and $N_0 = 2^\rho$. Due to the recursive structure of SCL decoding, the statistics of D_m are the same for all $N \geq N_0$ if the first N_0 frozen bits are the same. Thus, Corollary 4 remains valid if we replace (27) by*

$$\Pr \left\{ \frac{1}{N_0} |D_m - \bar{D}_m| > \beta \right\} \leq 2 \exp \left(-\frac{\beta^2}{2} N_0 \right).$$

This provides a significant improvement when $N_0 \ll N$. The same idea can also be applied to Corollary 3 but the value of δ must be modified as well.

Note that the bounds of the form (24) are typically loose (see [18, Sec. IV] for a discussion on tightness of the concentration results for the performance of a randomly chosen LDPC code around the ensemble average). Nevertheless, such analysis shows that the mean \bar{D}_m under consideration is meaningful.

V. SIMULATION RESULTS

This section provides simulation results for some constructions with dynamic frozen bits. In particular, we consider instances from an ensemble of modified RM codes, namely dynamic Reed–Muller (dRM) codes [22].

Definition 1. *The dRM(r, m) ensemble, denoted by $\mathcal{C}(r, m)$, is the set of all codes, specified by set \mathcal{A} of the RM(r, m) code and setting, for $i \in \mathcal{F}$,*

$$u_i = \begin{cases} \sum_{j \in \mathcal{A}^{(i-1)}} v_{j,i} u_j & \text{if } \mathcal{A}^{(i-1)} \neq \emptyset \\ 0 & \text{otherwise.} \end{cases}$$

with all possible $v_{j,i} \in \{0, 1\}$ and $\mathcal{A}^{(0)} \triangleq \emptyset$.

Recently, Arıkan introduced polarization-adjusted convolutional (PAC) codes [12], which can be represented as a polar code with dynamic frozen bits [29]. The rate-profiling choice of a PAC code is directly reflected in the frozen index set of its polar code representation [29]. Thus, if \mathcal{A} of an RM(r, m) code is chosen as the rate-profiling (as in [12]), then the corresponding PAC code becomes an instance from $\mathcal{C}(r, m)$. Another instance is the RM(r, m) code.

A. The Binary-Input Additive White Gaussian Channel

Fig. 1 shows simulation results for a random instance from $\mathcal{C}(3, 7)$ and a novel design (based on suggestions in Remark 2) under SCL decoding with $L = 2^{14}$ and $E_b/N_0 = 0.5$ together with the upper and lower bounds (6b) and (6a) on \bar{D}_m . The proposed code takes the set \mathcal{A}_{RM} of the (128, 64) RM code and obtains a new set as $\mathcal{A} = (\mathcal{A}_{\text{RM}} \setminus \{30, 40\}) \cup \{1, 57\}$, i.e., $u_{\{30, 40\}}$ are frozen and $u_{\{1, 57\}}$ are unfrozen, where each frozen bit is still set to a random linear combination of preceding information bit(s). Fig. 1 validates the bounds (6a),

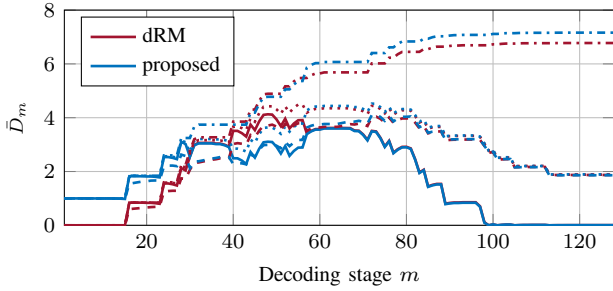


Fig. 1. \bar{D}_m vs. m at $E_b/N_0 = 0.5$ dB for (128, 64) codes (dash-dotted: upper bound (6b), solid: lower bound (6a), dotted: \bar{D}_m via simulation, dashed: $\mathbb{E}[\log_2 |\mathcal{S}_{0.94}^{(m)}|]$ via simulation).

(6b), (7) and (8). Note that we set the parameter $\alpha = 0.94$ in (7) to provide a robust estimate by capturing the near misses, which happen if there are decoding paths with probabilities slightly larger than that of the correct path. To understand this better, consider the proposed design where u_1 is an information bit. If one sets $\alpha = 1$, we get

$$\mathbb{E} \left[\log_2 |\mathcal{S}_1^{(1)}| \right] \approx 0.5 \log_2 1 + 0.5 \log_2 2 = 0.5 \quad (28)$$

which follows from $\bar{D}_m \approx 1$. Observing Fig. 1, we obtain $\mathbb{E} \left[\log_2 |\mathcal{S}_{0.94}^{(1)}| \right] \approx 1$. Therefore, tightness of (7), especially at early decoding stages, is impacted by the choice of α .⁴ Our numerical results show that the curve for $\mathbb{E} \left[\log_2 |\mathcal{S}_\alpha^{(m)}| \right]$ is more robust to changes in α at late decoding stages, i.e., for larger values of m . This means that the near misses happen at early decoding stages more often. In addition, observe that (6a) closely tracks the simulation for $m \leq 50$ and it is easy to compute via standard methods, e.g., we used Gaussian approximation of density evolution [30], which further motivate using it for code design. Following Remark 2, we chose a relatively small E_b/N_0 for the analysis, e.g., close to the Shannon limit (~ 0.189 dB) for rate- $1/2$ codes, since we are after the rare-event probabilities.

The changes leading to the new design help especially for the considered list size $L = 32$ by inspecting Fig. 2. The proposed code outperforms the dRM code especially at higher SNR values with this list size. The reason is illustrated by the lower bounds on \bar{D}_m in Fig. 1. In addition to having a smaller peak value, this peak occurs for the proposed design later than for the dRM code. This helps for the proposed code to not lose the correct path at early decoding stages, and hence, to keep it in the list towards the end for small list sizes, e.g., $L = 32$. If the list size is further decreased, then having u_1 as information bit can cause a degradation.⁵ This validates the analysis illustrated in Fig. 1. The performance for the 5G design employing the CRC-11 defined by the generator polynomial $g(x) = x^{11} + x^{10} + x^9 + x^5 + 1$ [5, Sec. 5.1], [31] under SCL decoding with $L = 32$ is 0.4 dB worse than the proposed design at a BLER around 10^{-4} . When SCL decoding with $L = 128$ is considered, both codes outperform the 5G

⁴One may further reduce the threshold α for inclusion to find a better match of $\mathbb{E} \left[\log_2 |\mathcal{S}_\alpha^{(m)}| \right]$ to \bar{D}_m for the entire range.

⁵In particular, if $L = 1$, (28) suggests that the correct path would be lost roughly half of the time already after first decoding stage.

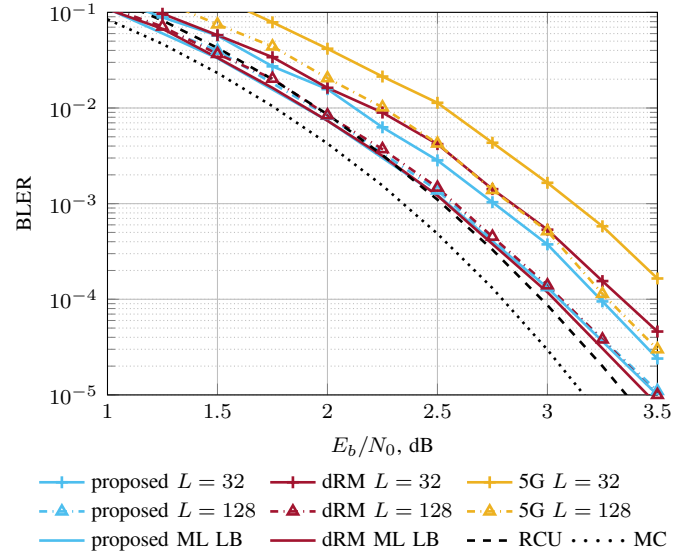


Fig. 2. BLER vs. SNR for (128, 64) codes.

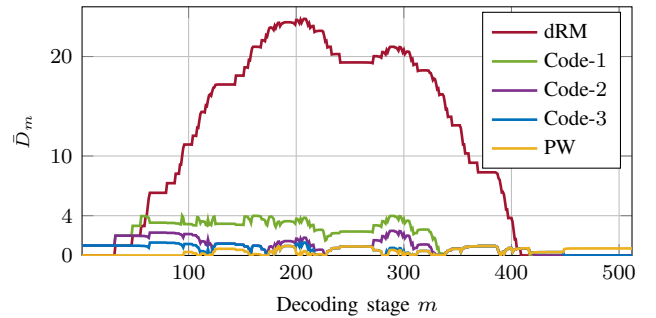


Fig. 3. Lower bound (6a) on \bar{D}_m vs. m at $E_b/N_0 = 0.5$ dB for (512, 256) codes.

design by no less than 0.25 dB at all BLERs considered. In particular, they perform within 0.15 dB of the random coding union (RCU) bound [32, Thm. 16] at the BLER of 10^{-5} and they almost match the simulation-based ML lower bounds [3], denoted as ML LB in the figure. Note that the PAC code perform very close to the dRM code under SCL decoding with $L \in \{32, 128\}$ [29, Fig. 1]. The metaconverse (MC) bound [32, Thm. 28] is also provided.

Next, consider moderate-length codes, e.g., (512, 256) codes, which are more challenging to design if the decoders are restricted to be of low- to moderate-complexity, i.e., $L \leq 1024$ [4, Sec. 5.2] [33]. Fig. 3 provides the bounds (6a) for dRM codes and three novel designs. The peak of the lower bound corresponding to the dRM code gets close to 25 and recall that this quantity is related to the logarithm of the required list size on average. This explains why SCL decoding needs very large list sizes for a good performance when used for the RM(4, 9) (or a dRM(4, 9)) code [34]. At the other extreme, the lower bound is provided for the construction based on the polarization weight (PW) method with $\beta = 2^{1/4}$ [35], which is more suitable for SCL decoding with small list sizes. The idea behind the designs is similar to the length-128 case: we start from the information positions of an RM code, modify the positions to lower the peak value and keep the curve flat so that there is enough entropy kept on the list to

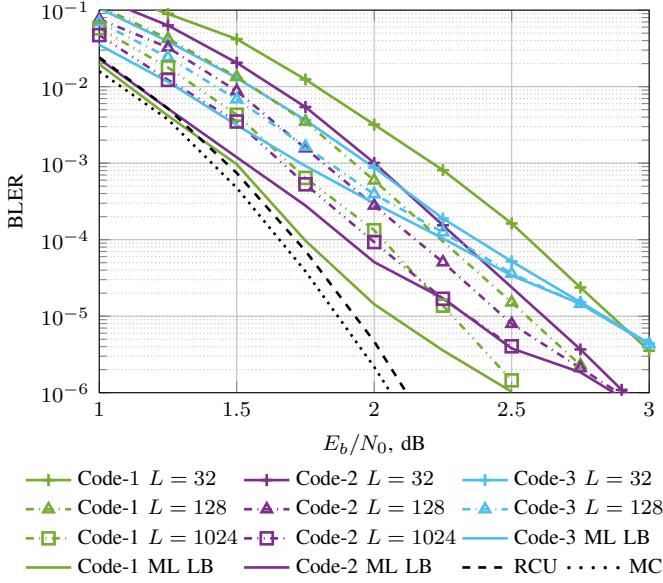


Fig. 4. BLER vs. SNR for (512, 256) codes.

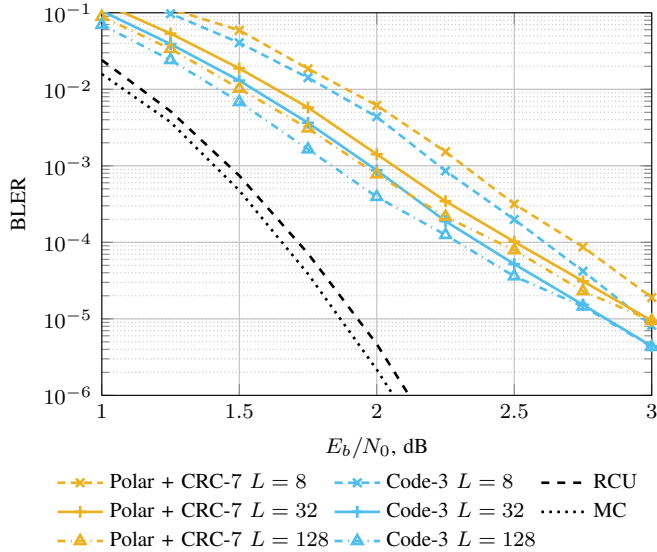


Fig. 5. BLER vs. SNR for (512, 256) concatenated polar codes with CRC-7 compared to Code-3.

make use of reliable frozen positions for a good performance. To this end, we also introduced u_1 as information bit in all three designs. This would harm the performance if the list size is very small, e.g., $L \leq 4$. In modifying the designs, we used the information positions from the PW construction. The information positions for the designs are provided in the appendix.

Fig. 4 compares the performance of three designs under different list sizes. Code-1 requires the largest list size to get closer to its ML performance. When a large list size is adopted, e.g., $L \in \{1024\}$, it performs within 0.4 dB of the RCU bound at BLERs around 10^{-6} , outperforming the non-binary LDPC code defined over \mathbb{F}_{256} which has a higher decoding complexity [33]. Nevertheless, even with $L = 1024$, there is a non-negligible gap to the ML lower bound at BLERs above 10^{-6} . Code-2 is competitive for a wide range of list

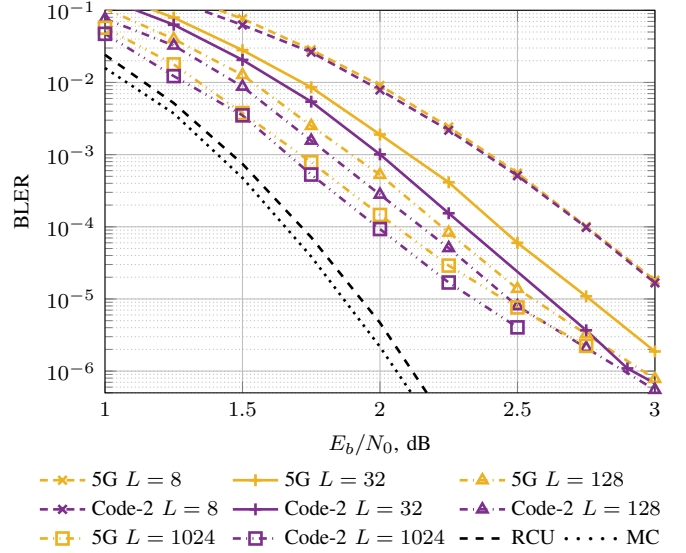


Fig. 6. BLER vs. SNR for (512, 256) 5G codes compared to Code-2.

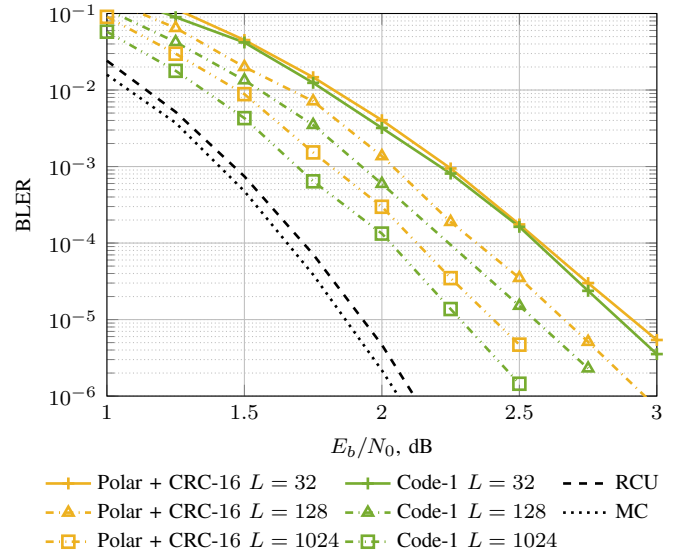


Fig. 7. BLER vs. SNR for (512, 256) concatenated polar codes with CRC-16 compared to Code-3.

sizes, i.e., $L \in [8, 1024]$. In particular, it performs within 0.75 dB from the RCU bound down to the BLER of 10^{-6} under SCL decoding with $L = 32$, outperforming the 5G design employing the CRC-11 with the generator polynomial $g(x) = x^{11} + x^{10} + x^9 + x^5 + 1$ by around 0.2 dB under the same list size at a BLER close to 10^{-6} (see Fig. 6). For $E_b/N_0 \geq 2.75$, Code-2 under SCL decoding with $L = 32$ performs as good as the 5G design under SCL decoding with $L = 128$. When an even smaller list size considered, e.g., $L = 8$, then Code-2 and the 5G design are indistinguishable while Code-3, which is expected to require smaller list sizes to approach its ML performance (see Fig. 3), outperforms them at all BLERs as can be seen in Fig. 5, where it is also compared to a polar code concatenated with the CRC-7 with the generator polynomial $g_7(x) = x^7 + x^6 + x^5 + x^2 + 1$.

⁶The polynomial is taken from [8] as it provides the best performance for the (128, 64) case although it may not be optimal for the (512, 256) code.

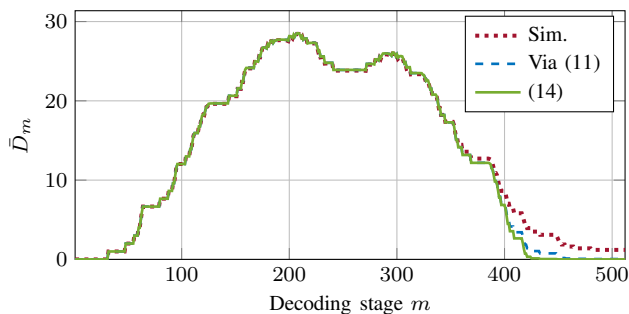


Fig. 8. \bar{D}_m vs. m at $\epsilon = 0.48$ for an instance from $\mathcal{C}(4,9)$.

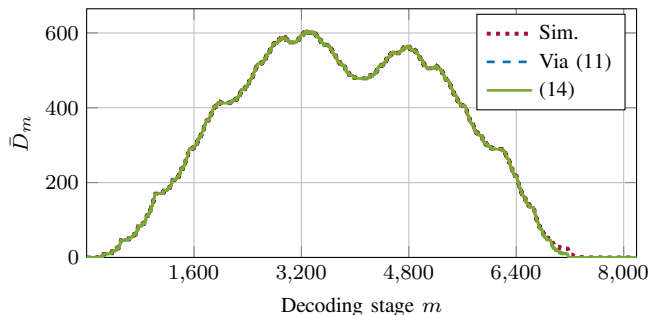


Fig. 9. \bar{D}_m vs. m at $\epsilon = 0.48$ for an instance from $\mathcal{C}(6,13)$.

With a relatively small list size, e.g., $L = 32$, Code-3 reaches to its ML performance at the BLER of 10^{-5} or less. Fig. 7 compares Code-1 to a polar code concatenated with the CRC-16 specified in [5, Sec. 5.1] with the generating polynomial $g_{16}(x) = x^{16} + x^{12} + x^5 + 1$. For the considered list sizes, Code-1 outperforms the modified polar code. In addition, Code-1 performs very similar to the 5G design when $L = 128$, it provides sizeable gains, e.g., 0.35 dB, at BLERs close to 10^{-6} when $L = 1024$. Note finally that for all polar codes (irrespective of the chosen CRC length) provided as reference in this work the indices of frozen bits are selected according to the 5G standard [5, Sec. 5.1], [31].

B. The Binary Erasure Channel

To understand the accuracy of the analysis and approximations presented in Sections III and IV, we simulated SCI decoding with consolidations for a *dRM ensemble sequence*, where the ℓ -th ensemble in the sequence is defined to be $\mathcal{C}(\ell, 2\ell + 1)$. Observe that each ensemble in the sequence consists of rate- $1/2$ codes. Note that as the block length changes, a random instance from the corresponding ensemble is picked for the simulations and the numerical results are quite similar for different instances chosen randomly. These simulations provide realizations of the random process D_1, \dots, D_N and we compare their mean to the theoretical predictions (11) and (14) in Figs. 8 and 9 for the case of $N = 512$ and $N = 8192$, respectively. These results show that for a random code in $\mathcal{C}(\ell, 2\ell + 1)$ the simulation mean is close to the simple recursive formula given as (14). Observe also that the mean computed by approximating the probabilities via Markov model (11) matches the mean slightly better for large values of m . With an increasing blocklength, (11) and (14) match the simulations better for large values of m .

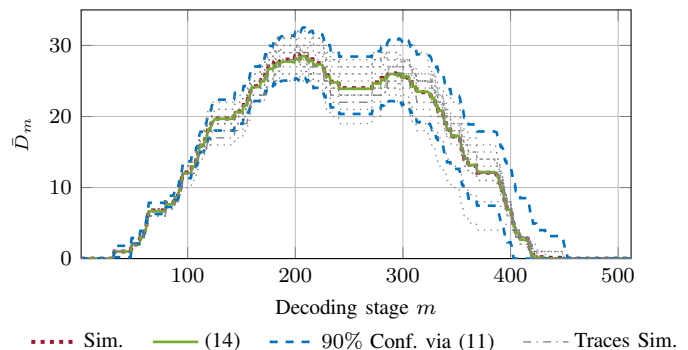


Fig. 10. \bar{D}_m vs. m for randomly permuted 246 erasures.

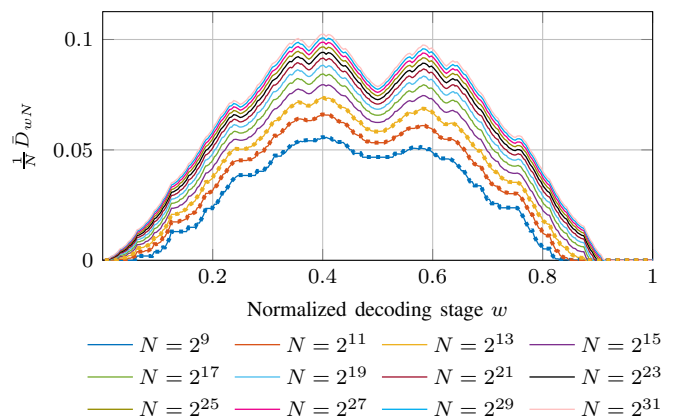


Fig. 11. $\frac{1}{N}\bar{D}_{wN}$ vs. w (solid: using (14) with an erasure probability $\epsilon = 0.48$, dashed: simulations for the fixed-weight BEC with $\text{round}(N\epsilon)$ erasures) for instances from dRM code ensembles $\mathcal{C}(\ell, 2\ell + 1)$, $\ell \in \{4, 5, \dots, 15\}$.

One weakness of these bounds is that the channel variation (e.g., in the number of erasures) significantly increases the variation in D_1^N , especially for small to medium blocklengths, e.g., recall Fig. 8 for the case of $N = 512$. To highlight the similarity between the theory and simulation even for such cases, we use a fixed-weight BEC that chooses a random pattern with exactly $\text{round}(N\epsilon)$ erasures. To motivate this, note that density evolution naturally captures the typical behavior of the analyzed system [28]. Fig. 10 shows that, even for the (512, 256) dRM code, the simulation mean is close to the analysis for the entire range of m . The 15 random simulation traces lie largely within the 90% confidence range of the Markov chain analysis (11).

Next, we study how the subspace dimension behaves as the block length increases for the introduced dRM ensemble sequence. Let $w \triangleq \frac{m}{N}$, $m \in [N]$, be the normalized decoding stage. Fig. 11 provides the normalized dimension $\frac{1}{N}\bar{D}_{wN}$ as a function of w for the samples of dRM ensemble sequence with different block lengths, from $N = 2^9$ up to $N = 2^{31}$. We stress again the accuracy of the analysis (14) validated by simulations up to $N = 2^{13}$ and we believe that the results for larger block lengths are also accurate. The asymptotic behavior of $\frac{1}{N}d_{wN}$ gives the asymptotic decoding complexity of an ML decoder implemented via SCI decoding. This provides insight into the asymptotic decoding complexity of RM codes to achieve the capacity over the BEC [36] for two reasons: first, RM code is a member of the ensemble, and second,

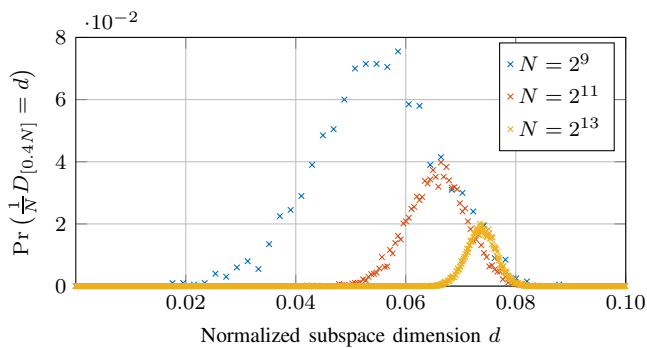


Fig. 12. $\Pr(\frac{1}{N}D_{[0.4N]} = d)$ vs. d for an erasure probability $\epsilon = 0.48$ for instances from dRM code ensembles $\mathcal{C}(\ell, 2\ell + 1)$, $\ell \in \{4, 5, 6\}$.

the simulation results look very similar for RM codes as well up to $N = 2^{13}$. Other decoding algorithms might give improvements on the complexity, but we are not aware of a lower-complexity ML decoder than SCI decoding for RM codes in the case of the BEC. Fig. 11 shows that the convergence seems to be rather slow for the defined sequence. Interesting directions include understanding what happens to $\frac{1}{N}\bar{D}_{wN}$ as $N \rightarrow \infty$ analytically and trying to define code sequences where $\max_w \frac{1}{N}\bar{D}_{wN}$ is significantly smaller than that of dRM codes, but still perform competitively.

Next, Fig. 12 provides the p.m.f. for $\frac{1}{N}D_{[0.4N]}$, where $[wN]$ is the nearest integer to wN , $w \in (0, 1]$. The parameter w is set to 0.4 since the mean analysis given in Fig. 11 shows that, for the considered codes, the mean reaches to its maximum around $w = 0.4$. Interestingly, the p.m.f.s concentrate around the mean $\frac{1}{N}\bar{D}_{[0.4N]}$ with increasing block length.

Finally, Fig. 13 compares the ML decoding performance of Code-1 designed in Section V-A to that of the RM(4, 9) and a random instance from $\mathcal{C}(4, 9)$ under SCI decoding.⁷ We declare an error whenever the linear system corresponding to the channel output does not provide a unique solution. The code performs as well as the RM(4, 9) code for frame error rates equal to 10^{-5} or higher with much lower average subspace dimension during decoding as illustrated in Fig. 14. Thus, we can match random code performance (like dRM) down to the BLER of 10^{-4} while performing well with smaller number of inactivations (i.e., shorter list sizes). For BLER of 10^{-5} or less, it experiences more severe error floor compared to the RM(4, 9) code. The Singleton bound [37] and the Berlekamp's random coding (BRC) bound [38] are provided as reference.

VI. CONCLUSION

In this paper, we consider the theoretical question ‘‘What list size suffices to achieve maximum-likelihood decoding performance under successive cancellation list (SCL) decoding?’’. The results identify information-theoretic quantities associated with the required list size on average and also lead to bounds

⁷Note that the performance for the (512, 256) RM and dRM codes were also provided in [22]. Here, we provide the performance curve for an exemplary construction in addition to Fig. 14, which illustrate the competitive performance of Code-1 for wide range of erasure probabilities while requiring much smaller subspace dimensions under SCI decoding with consolidations (or list lengths under SCL decoding) to achieve ML decoding.

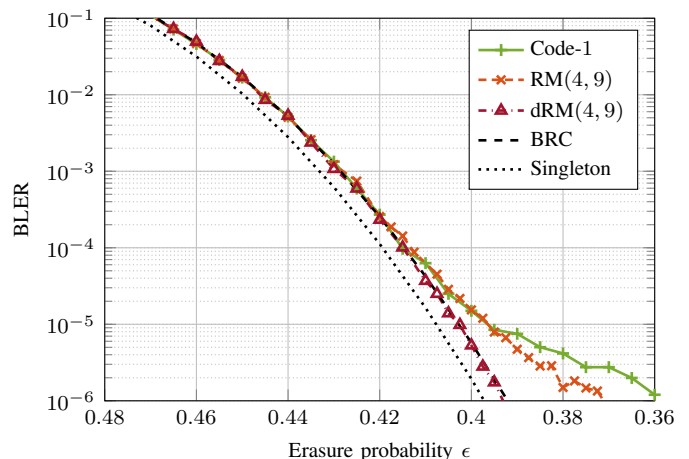


Fig. 13. BLER vs. ϵ for (512, 256) codes.

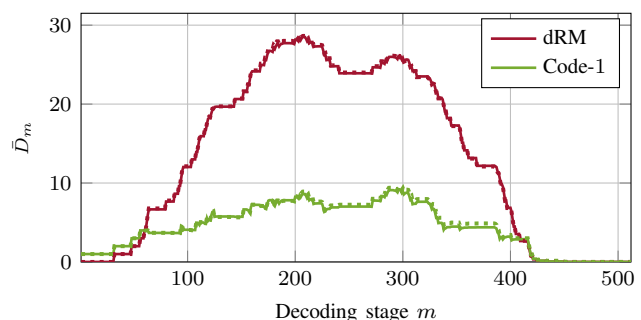


Fig. 14. \bar{D}_m vs. m for Code-1 compared to the RM code (solid: using (14) with an erasure probability of $\epsilon = 0.48$, dashed: simulations for the fixed-weight BEC with 246 erasures).

that can be computed efficiently even for very long codes. It has been shown that the logarithm of the random required list size concentrates around the mean. A simple and accurate recursive approximation of this mean is provided for the binary erasure channel (BEC).

Simulation results show that this approximation captures the dynamics of the required list size at each stage of decoding on the BEC. For general binary memoryless symmetric channels, e.g., binary-input additive white Gaussian noise (BIAWGN) channel, the analysis identified the key quantity \bar{D}_m as a proxy for the uncertainty in SCL decoding. The analysis suggested codes with improved performance under SCL decoding with various list sizes, e.g., $L \in [8, 1024]$, for short- to moderate-length codes, over the BIAWGN channel, although the work primarily aims at understanding SCL decoding from an information-theoretic perspective. Future work should devise a constructive algorithm which take into account the introduced quantities to design good codes for SCL decoding with practical list sizes for a wide range of block lengths, e.g., for $N \leq 2048$.

APPENDIX

A. The Designs for (512, 256) Case

Let \mathcal{A}_{PW} denote the set of information positions of the (512, 256) polar code designed according to PW with $\beta = 2^{1/4}$

[35]. The sets \mathcal{A}_1 , \mathcal{A}_2 and \mathcal{A}_3 corresponding to Code-1, Code-2 and Code-3, respectively, are given as follows:

$$\begin{aligned}\mathcal{A}_3 &= (\mathcal{A}_{\text{PW}} \setminus \{449, 450, 451, 453, 457, 465, 481\}) \\ &\quad \cup \{1, 64, 118, 122, 159, 200, 284\}, \\ \mathcal{A}_2 &= (\mathcal{A}_3 \setminus \{122, 421, 425, 433\}) \cup \{32, 174, 272, 280\}, \\ \mathcal{A}_1 &= (\mathcal{A}_2 \setminus \{64, 96, 125, 180, 418, 419\}) \\ &\quad \cup \{48, 56, 94, 108, 122, 152\}.\end{aligned}$$

For all codes, each frozen bit is set to a random linear combination of preceding information bit(s). The performance curves will also be available on [39].

ACKNOWLEDGEMENT

The authors thank Gerhard Kramer (TUM), the associate editor and anonymous reviewers for comments improving the presentation.

REFERENCES

- [1] M. C. Coşkun and H. D. Pfister, "Bounds on the list size of successive cancellation list decoding," in *2020 Int. Conf. on Signal Process. and Commun. (SPCOM)*, 2020, pp. 1–5.
- [2] E. Arıkan, "Channel polarization: A method for constructing capacity-achieving codes for symmetric binary-input memoryless channels," *IEEE Trans. Inf. Theory*, vol. 55, no. 7, pp. 3051–3073, Jul. 2009.
- [3] I. Tal and A. Vardy, "List decoding of polar codes," *IEEE Trans. Inf. Theory*, vol. 61, no. 5, pp. 2213–2226, May 2015.
- [4] M. C. Coşkun, G. Durisi, T. Jerkovits, G. Liva, W. Ryan, B. Stein, and F. Steiner, "Efficient error-correcting codes in the short blocklength regime," *Elsevier Phys. Commun.*, vol. 34, pp. 66–79, Jun. 2019.
- [5] *Technical Specification Group Radio Access Network - NR - Multiplexing and channel coding*, 3GPP Technical specification TS 38.212 V16.5.0, Mar. 2021.
- [6] P. Trifonov and V. Miloslavskaya, "Polar subcodes," *IEEE J. Sel. Areas Commun.*, vol. 34, no. 2, pp. 254–266, Feb. 2016.
- [7] P. Trifonov and G. Trofimiuk, "A randomized construction of polar subcodes," in *Proc. IEEE Int. Symp. Inf. Theory*, 2017, pp. 1863–1867.
- [8] P. Yuan, T. Prinz, G. Böcherer, O. İşcan, R. Böhnke, and W. Xu, "Polar code construction for list decoding," in *Proc. 11th Int. ITG Conf. on Syst., Commun. and Coding (SCC)*, Feb. 2019, pp. 125–130.
- [9] A. Elkelesh, M. Ebada, S. Cammerer, and S. ten Brink, "Decoder-tailored polar code design using the genetic algorithm," *IEEE Trans. Commun.*, vol. 67, no. 7, pp. 4521–4534, 2019.
- [10] A. Fazeli, A. Vardy, and H. Yao, "Convolutional decoding of polar codes," in *IEEE Int. Symp. on Inf. Theory*, 2019, pp. 1397–1401.
- [11] M. Rowshan and E. Viterbo, "How to modify polar codes for list decoding," in *IEEE Int. Symp. Inf. Theory*, Jul. 2019, pp. 1772–1776.
- [12] E. Arıkan, "From sequential decoding to channel polarization and back again," *CoRR*, vol. abs/1908.09594, 2019. [Online]. Available: <http://arxiv.org/abs/1908.09594>
- [13] V. Miloslavskaya and B. Vucetic, "Design of short polar codes for SCL decoding," *IEEE Trans. Commun.*, vol. 68, no. 11, pp. 6657–6668, 2020.
- [14] P. Trifonov, "Randomized polar subcodes with optimized error coefficient," *IEEE Trans. Commun.*, vol. 68, no. 11, pp. 6714–6722, 2020.
- [15] I. Reed, "A class of multiple-error-correcting codes and the decoding scheme," *Trans. IRE Prof. Group on Inf. Theory*, vol. 4, no. 4, pp. 38–49, Sep. 1954.
- [16] D. E. Muller, "Application of boolean algebra to switching circuit design and to error detection," *Trans. IRE Prof. Group on Electronic Computers*, vol. EC-3, no. 3, pp. 6–12, Sep. 1954.
- [17] M. G. Luby, M. Mitzenmacher, M. A. Shokrollahi, and D. A. Spielman, "Analysis of low density codes and improved designs using irregular graphs," in *Proc. ACM Symp. on Theory of Computing*, ser. STOC '98. New York, NY, USA: Association for Computing Machinery, 1998, p. 249–258. [Online]. Available: <https://doi.org/10.1145/276698.276756>
- [18] T. J. Richardson and R. L. Urbanke, "The capacity of low-density parity-check codes under message-passing decoding," *IEEE Trans. Inf. Theory*, vol. 47, no. 2, pp. 599–618, 2001.
- [19] N. Stolte, "Rekursive Codes mit der Plotkin-Konstruktion und ihre Decodierung," Ph.D. dissertation, TU Darmstadt, 2002.
- [20] I. Dumer and K. Shabunov, "Near-optimum decoding for subcodes of Reed-Muller codes," in *Proc. IEEE Int. Symp. Inf. Theory*, Jun. 2001, p. 329.
- [21] J. Neu, "Quantized polar code decoders: Analysis and design," *CoRR*, vol. abs/1902.10395, 2019. [Online]. Available: <http://arxiv.org/abs/1902.10395>
- [22] M. C. Coşkun, J. Neu, and H. D. Pfister, "Successive cancellation inactivation decoding for modified Reed-Muller and eBCH codes," in *IEEE Int. Symp. Inf. Theory*, Jun. 2020, pp. 437–442.
- [23] A. Shokrollahi, "Raptor codes," *IEEE Trans. Inf. Theory*, vol. 52, no. 6, pp. 2551–2567, Jun. 2006.
- [24] C. Measson, A. Montanari, and R. Urbanke, "Maxwell construction: The hidden bridge between iterative and maximum a posteriori decoding," *IEEE Trans. Inf. Theory*, vol. 54, no. 12, pp. 5277–5307, Dec. 2008.
- [25] A. Eslami and H. Pishro-Nik, "On bit error rate performance of polar codes in finite regime," in *Proc. Allerton Conf. on Commun., Control, and Comput.*, Sep. 2010, pp. 188–194.
- [26] S. A. Hashemi, M. Mondelli, S. H. Hassani, C. Condo, R. L. Urbanke, and W. J. Gross, "Decoder partitioning: Towards practical list decoding of polar codes," *IEEE Trans. Commun.*, vol. 66, no. 9, pp. 3749–3759, 2018.
- [27] M. Mitzenmacher and E. Upfal, *Probability and Computing: Randomized Algorithms and Probabilistic Analysis*. USA: Cambridge University Press, 2005.
- [28] T. Richardson and R. Urbanke, *Modern Coding Theory*. New York, NY, USA: Cambridge University Press, 2008.
- [29] H. Yao, A. Fazeli, and A. Vardy, "List decoding of arıkan's pac codes," *Entropy*, vol. 23, no. 7, 2021. [Online]. Available: <https://www.mdpi.com/1099-4300/23/7/841>
- [30] P. Trifonov, "Efficient design and decoding of polar codes," *IEEE Trans. Commun.*, vol. 60, no. 11, pp. 3221–3227, Nov. 2012.
- [31] V. Bioglio, C. Condo, and I. Land, "Design of polar codes in 5G new radio," *IEEE Commun. Surveys Tutorials*, vol. 23, no. 1, pp. 29–40, 2021.
- [32] Y. Polyanskiy, V. Poor, and S. Verdù, "Channel coding rate in the finite blocklength regime," *IEEE Trans. Inf. Theory*, vol. 56, no. 5, pp. 2307–235, May 2010.
- [33] O. İşcan, D. Lentner, and W. Xu, "A comparison of channel coding schemes for 5G short message transmission," in *IEEE Global Commun. Conf. Workshops*, 2016, pp. 1–6.
- [34] M. Mondelli, S. H. Hassani, and R. L. Urbanke, "From polar to Reed-Muller codes: A technique to improve the finite-length performance," *IEEE Trans. Commun.*, vol. 62, no. 9, pp. 3084–3091, Sep. 2014.
- [35] G. He, J. Belfiore, I. Land, G. Yang, X. Liu, Y. Chen, R. Li, J. Wang, Y. Ge, R. Zhang, and W. Tong, "Beta-expansion: A theoretical framework for fast and recursive construction of polar codes," in *IEEE Global Commun. Conf.*, 2017, pp. 1–6.
- [36] S. Kudekar, S. Kumar, M. Mondelli, H. D. Pfister, E. Şaşıoğlu, and R. L. Urbanke, "Reed-Muller codes achieve capacity on erasure channels," *IEEE Trans. Inf. Theory*, vol. 63, no. 7, pp. 4298–4316, Jul. 2017.
- [37] R. Singleton, "Maximum distance q-ary codes," *IEEE Trans. Inf. Theory*, vol. 10, no. 2, pp. 116–118, Apr. 1964.
- [38] E. R. Berlekamp, "The technology of error-correcting codes," *Proc. IEEE*, vol. 68, no. 5, pp. 564–593, May 1980.
- [39] G. Liva and F. Steiner, "pretty-good-codes.org: Online library of good channel codes," <http://pretty-good-codes.org>, Mar. 2021.